Peri-Implant Strain in an In Vitro Model

Souheil Hussaini, BDS, MS[1]
Tritala K. Vaidyanathan, BSc, BE, MASc, PhD[2]
Abhinav P. Wadkar, BDS, MS[2]
Firas A. Al Quran, BDS, MSc Med, PhD[3]
David Ehrenberg, DDS, MS[2]
Saul Weiner, DDS[2]*

An in vitro experimental model was designed and tested to determine the influence that peri-implant strain may have on the overall crestal bone. Strain gages were attached to polymethylmethacrylate (PMMA) models containing a screw-type root form implant at sites 1 mm from the resin-implant interface. Three different types of crown superstructures (cemented, 1-screw [UCLA] and 2-screw abutment types) were tested. Loading (1 Hz, 200 N load) was performed using a MTS Mechanical Test System. The strain gage data were stored and organized in a computer for statistical treatment. Strains for all abutment types did not exceed the physiological range for modeling and remodeling of cancellous bone, 200–2500 με (microstrain). For approximately one-quarter of the trials, the strain values were less than 200 με the zone for bone atrophy. The mean microstrain obtained was 517.7 με. In conclusion, the peri-implant strain in this in vitro model did not exceed the physiologic range of bone remodeling under axial occlusal loading.

Key Words: dental implants, bone strain, abutments, strain gages, stress shielding, microstrain

INTRODUCTION

While the use of endosseous implants has achieved success rates that are generally greater than 95%,[1] the issue of crestal bone resorption continues to receive significant interest from both researchers and clinicians. There are a number of theories to explain this phenomenon, including the following: the trauma associated with second stage surgery,[2] plaque-associated peri-implantitis,[3] excessive force transfer associated with occlusal loads during tooth contact,[4] the inability of the rigid bone-implant interface to absorb physiologic forces without a periodontal ligament—particularly when the bone is thin, and stress shielding.[5,6,7,8] These conflicting hypotheses suggest that a basic understanding of the mechanisms underlying crestal bone changes is still lacking, since occlusal forces for patients with implant-supported restorations appear to be within the range of the masticatory forces observed in the natural dentition.[6,9]

Both in vitro photoelastic studies and finite element computer modeling suggest that the crestal bone receives significant shear stress, particularly in cortical areas. Nonetheless, Pilliar and others[10,11] claim that, at least under some circumstances, the crestal bone is stress shielded and receives an inadequate stimulus to maintain bone volume.

Martin and Burr[12] and Frost[13] categorize the effect of compressive strain on bone as demonstrating a physiological modeling-remodeling zone between 200 and 2500 με, an overload zone between 2500 and 4000 με (where damage and microcracking of the bone occurs with some repair), and finally a pathological overload zone of strains greater than 4000 με where little or no repair of the bone is observed. Furthermore, Mori and Burr[14] show that microdamage can be identified in areas of active remodeling.

Application of these observations to the dental implant-bone interface suggests this as a mechanism to explain the repair of the crestal interface from fatigue-induced microdamage. For example, Hoshaw et al[15] observed an increase in both the modeling and remodeling responses with a net bone loss near the coronal portion of the loaded implants. Another mechanism suggested is that abutment movement on the implant creates strain in the peri-implant crestal bone by distortion of the collar of the implant.[16] However, other investigators suggest stress shielding—that is, a lack of adequate strain in the crestal bone—as an explanation for the resorption seen in the crestal bone.[17,18]

The purpose of these experiments was to examine the magnitude of the strains in the crestal bone adjacent to the machined collar of a dental implant in an in vitro model system.

METHODS

The overall experimental strategy was to develop an in vitro system in which a strain gage was located proximal to the crestal area of the implant to measure the strain from occlusal loading.

Model fabrication

We constructed a wax pattern of a box 20 mm long, 10 mm wide, and 15 mm high with an open top and containing a hollow wax cylinder with inner diameter of 5 mm and a wall

[1] Oral Implantology Research Institute, Dubai, UAE.
[2] Department of Restorative Dentistry, Rutgers School of Dental Medicine, Newark, NJ.
[3] University of Sharjah, UAE; Jordan University of Science and Technology, Irbid, Jordan.
* *Corresponding Author*, e-mail: forasaul@aol.com
DOI: 10.1563/AAID-JOI-D-12-00305

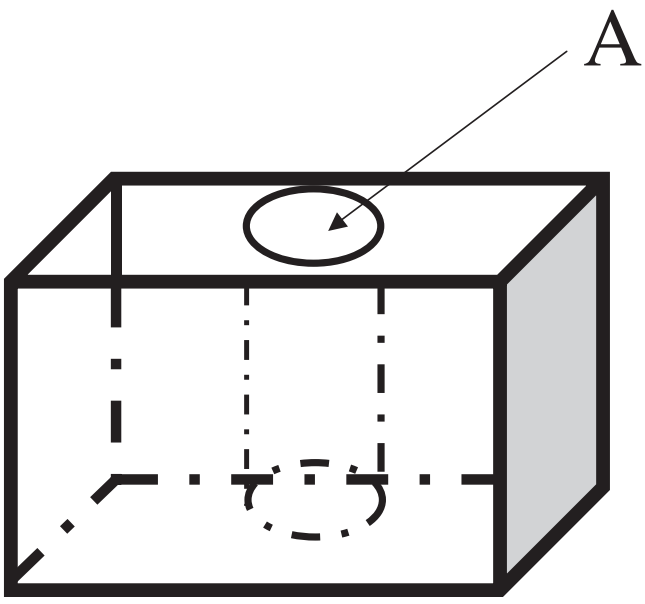

Figure 1. Schematic of the resin box used to stabilize the implant and attach the strain gages. (a) The resin tube into which the implant is inserted. The strain gages were attached to the outer walls of the tube. Following this, the box was filled with resin.

thickness of 1 mm (Figure 1). It was invested in an elastic polyvinylsiloxane material (Reprosil, Dentsply International Inc, Milford, Del) to obtain a mold. Polymethylmethacrylate (PMMA) was utilized as the material in which the implants were embedded because it has a modulus of elasticity similar to that of cancellous bone,[19–22] 1.3–2.0 GPa;[23] therefore, it is analogous to clinical situations in which implants are placed into Type 2 and Type 3 osseous beds.[24] A mixture of PMMA resin monomer liquid and polymer powder (Lang Dental Mfg Co, Wheeling, Ill) in a ratio of 1:1.5 was poured into the mold and allowed to cure under 20 psi in warm water for 15 minutes. Five samples were made.

Cementation of implants and strain gages

Branemark Mark II, 4 mm diameter × 10 mm length, implants (Nobel Biocare Inc, Yorba Linda, Calif) were cemented into the cylinder of each experimental sample flush with the top using a jig from a surveyor (Ney Dental International, Bloomfield, Conn), such that the implant was placed perpendicular to the floor of the sample using a 1:1.5 mixture of acrylic resin monomer and polymer. Following polymerization, the PMMA coating around the implant surface was shaved with a milling machine (Cenders & Netaux SA, Bienne, Switzerland) to a 1 mm thickness to allow the positioning of the strain gages proximal to the implant in the crestal area (Figure 2).

Strain gages, type EA-06-062AQ-350 (Measurements Group, Inc, Raleigh, NC) were cemented on the buccal, mesial, and distal surfaces of each resin cylinder using cyanoacrylate cement (Measurements Group, Inc, Raleigh, NC) following the manufacturer's standard protocols. Following this, a 3 mm–thick layer of PMMA was applied uniformly over the strain gages to simulate the clinical situation where there is generally a minimum of 3 mm of bone between an implant and the neighboring tooth or implant. Embedding has no effect on the data recorded from the strain gages[25,26] (Figure 3).

Abutments and crowns

Three types of abutment systems were utilized:

1. Standard abutment with a cemented crown;
2. UCLA abutment crown cast as one unit;
3. Screw-retained crown with a separate abutment (Esthetic-Cone abutment and cast-to coping, NobelBiocare, Yorba Linda, Calif).

Standard laboratory procedures were used for fabrication of each crown. The superstructures for all 3 abutment systems had the same occluso-gingival, buccolingual, and mesiodistal dimensions, simulating a premolar. The height of the occlusal surface of the crowns measured 9 mm from the implant-abutment interface. One set of crowns was fabricated and utilized for all 5 samples to eliminate variability in the crown superstructure.

Occlusal loading protocol

Each of the samples was mounted onto a Dental Materials Testing System (Model #810, MTS System Corp, Minneapolis, Minn), a computer-guided simulated oral environment where occlusal loading (Figure 4) against a natural premolar loading was cyclic, 1 Hz, at 200 N, along the long axis of the implant to simulate vertical chewing[27] (Figure 4).

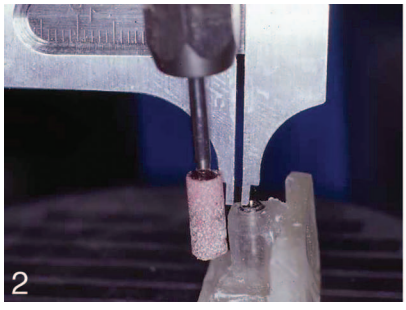

Figure 2–4. Figure 2. An experimental sample prior to placing the strain gages. The walls of the resin cylinder containing the implant are being reduced to a thickness of 1 mm. **Figure 3.** A completed specimen with the strain gages attached. The implant is in the center of the sample. The leads from the strain gages attached to the acrylic extend outward from the sample. **Figure 4.** The MTS system with loaded sample.

TABLE 1

Mean microstrain values for the three abutment types

Abutment type	Number of samples	Mean value in με
1-screw (UCLA)	45	596.7*
2-screw	45	462.4*
Cemented	45	386.4*

*$P \leq .0001$

Data collection

The signals from the strain gages were passed through a Model 2120A Strain Gage Conditioner/Amplifier (Measurements Group, Raleigh, NC) to a GraphTec WR7700 chart recorder (Schindler Elevator Corp, Randolph, NJ) at an acquisition rate of 32 Hz. The distal, mesial, and buccal strain gage outputs and the load sensor output from the MTS machine were recorded.

The load signal was sinusoidal with constant amplitude for each set of nine cycles with a frequency of 1 Hz. The data used for analysis included the peak values of the strain gage signal on the chart recorder for each sample run. A conversion factor was used to transform the chart peak values from millimeters into strain units using a calibration resistor in the 2120 signal conditioning unit (31 mm / 951 Micro-Strain). The calibration resistor is a fixed value resistor switched into either arm of a Wheatstone bridge to balance the circuit, giving a 951 με value with an excitation voltage of 2 volts and a gage factor of 2.125. The strain signal was then routed through a data acquisition board interface (A/D converter) connected to a personal computer, and transferred into a file for analysis.

Statistical analysis

1. The data was first subjected to a chi-square analysis by dichotomizing it into 2 groups. The first included strains between 0 and +200 με. The second included strains ≥200 με. The analysis was cross-tabulated with abutment type.
2. A general linear model (GLM) procedure ANOVA for unbalanced data was used to compare the mean strains between abutment types by isolating the large experimental error due to trial-to-trial variations and placement of the gages among the 5 samples. Posthoc pair-wise comparisons were made using Tukey's protected t-test.[28]

RESULTS

The mean microstrain values for the trials with the 3 different abutment types were as follows: 596.7 με for the1-screw (UCLA) abutment type, 462.4 με for the 2-screw abutment type, and 386.4 με for the cemented abutment type.

When the data were dichotomized by microstrain values, 73.33% of the trials were within the physiologic range for the 1-screw (UCLA) abutment type, 76.3% for the 2-screw abutment type, and 68.89% for the cemented abutment type. The remaining trials for each of the abutment types were within the disuse atrophy range. No trials with microstrain values greater than 2500 με were observed (Table 1).

TABLE 2

Effects of abutment type on peri-implant strains*

Abutment type	Number of samples	Percentage within physiologic range	Mean strain values in με-(*SD*)
1-screw (UCLA)	45	73.33%	596.7 (682.5)
2-screw	45	76.30%	462.4 (336.3)
Cemented	45	68.89%	386.4 (253.4)

*Fisher's exact test (2-tail) $P = .397$. Standard error ± 4.33%. Total number of samples = 135.

TABLE 3

Ranking by abutment type utilized in nonparametric analysis

Abutment type	Number of samples	Average rank
1-screw (UCLA)	45	211.4*
2-screw	45	209.2*
Cemented	45	188.4*

*$P \leq .0001$

Chi-square analysis

Comparison of the dichotomized data for the 3 different abutment types using Fisher exact test showed that the percentage of trials where the measured strains 1 mm from the implant-resin interface were within the physiological range were statistically the same for all three groups (Table 2).

Analysis of variance

Statistically significant differences were found between mean peri-implant strains observed with the 3 abutment types ($P < .05$). The 1-screw (UCLA) abutment type demonstrated the highest peri-implant strains. The 2-screw abutment type had an intermediate level of strains 1 mm from the implant-resin interface, while the cemented abutment type had the lowest strains. The ANOVA is shown in Table 3. No statistical differences were found in the data recorded from the buccal, mesial, and distal gages; thus, the data from the 3 sites were combined. Because of the large variation among samples, an additional nonparametric analysis—the Wilcoxan signed-rank test—was performed and demonstrated similar results (Table 4).

DISCUSSION

These experiments demonstrate that, in this in vitro system, normal masticatory loads resulted in strains within the physiological capacities of peri-implant bone to remodel and maintain its integrity. In these experiments, 73% of the recorded microstrain values were categorized as within the physiological range, 200–2500 με, while the remainder fell in the subphysiological range of 0–200 με. Loads in the latter range could result in resorption associated with disuse atrophy.[29] These results are based on masticatory loads of 200 N. Many individuals, however, function with masticatory loading that are less than 200 N,[30–34] which could lead to a reduced strain that is associated with disuse atrophy. That being said, loading of the samples in these experiments was

centered over the long axis of the fixture. Eccentric loading might result in magnification of the microstrain. This would be especially true in situations where the implant superstructure includes cantilevered units that would magnify the effects of the applied load, particularly in the crestal bone adjacent to the cantilever.[35]

There is considerable uncertainty regarding the etiology of the 1–1.5 mm of crestal bone loss commonly seen in the first year after implants are loaded. A number of photoelastic studies[36–38] claim that relatively high levels of strain occur in the peri-implant crestal area. In support of these studies, finite element modeling studies by Borchers et al,[39] Cook et a1,[40] and Misch et al[41] make similar predictions. Another explanation to support the hypothesis of high stress levels in the peri-implant area is based on the observation that there is a very significant discrepancy—10 times order of magnitude—between the modulus of elasticity of bone and that of the titanium fixture.[42] As a result, relative motion is generated between the implant (made of titanium) and the bone, which flexes because of its lower modulus. Thus, high levels of strain may be generated in the bone. No experimental evidence, however, is currently available to support this theory.

A second contrasting theory presented by Pillar et al,[31,43,16] with both experimental histological evidence and finite element modeling, claims that stress shielding occurs in the peri-implant crestal bone resulting in disuse atrophy. This does not exclude the possibility that in some circumstances with long cantilevers or short implants, excessive strain may lead to microfracture and destruction of the peri-implant bone.[35]

Vaillancourt et al,[18] who proposed that the loss of crestal peri-implant bone observed in the first year of loading is a result of disuse atrophy, estimate on the basis of finite element analysis that a minimum load of 153 N on the implant is needed to produce an adequate strain in the crestal peri-implant bone to stimulate physiologic remodeling and prevent disuse atrophy.

Loading of the 3 different abutment systems resulted in statistical differences in the peri-implant crestal strains. The 1-screw (UCLA) system showed the highest strains at 596.7 με; the 2-screw measured an intermediate strain at 462.4 με; and the lowest stress transmission was observed around the cemented abutment at 386.4 με. It has been suggested that the gold screw of the 2-screw system served to reduce the load transferred to the implant-resin interface.[44] With these micro-strain values, however, it is possible that both the gold screw and the cement layer reduced the stress transmission.

While the large standard deviations of the sample mean is disappointing, the strain records obtained during cyclic loading of each implant sample were consistent in each group of trials. The large intertrial variance was controlled by use of the GLM procedure, ANOVA, and the application of a nonparametric analysis. Most importantly, however, the large variability in the standard deviation did not affect the major findings of the study: that is, there were no trials in which the mean values exceeded the 2500 microstrain limit of physiologic modeling and remodeling activity. Furthermore, Brennan et al[45] Wang and Stohler,[46] and Kaukinen et al[47] all demonstrate a wide inter-sample variation in their strain gage studies , similar to those observed in this research. This points to the sensitivity of the strain gage measuring systems and the difficulties associated with standardization of the samples.

The use of PMMA as a bone analogue has significant limitations. While Young's modulus for cancellous bone and PMMA are similar,[18–22,25] bone is an heterogenous substance composed of cortical bone, as well as trabecular bone with anisotropic properties.[48] PMMA, however, is a homogenous substance. Thus, extrapolation of the results of these experiments using PMMA to biologic systems must be approached with caution. It is more realistic to view these series of experiments as an initial study that should serve as the basis for more elaborate experimental methodologies that employ bone specimens and in vivo models.

There are a variety of surface treatments for the collar of the implant. These include machined, roughened (by etching, blasting, or oxidizing), and grooving. The stress transfer to the bone probably differs among them. This study examined the stress transfer from the machined collar. Further studies are needed to evaluate the effects of a more intimate interface between the collar of the implant and the bone, as occurs with a roughened or grooved surface. This does not, however, invalidate the results of the study; in fact, the differences—if indeed they exist—may be a partial explanation for the phenomenon of crestal bone loss. Another issue that requires further investigation is that of the effects of eccentric loading. This was a preliminary experiment to present an approach other than FEA to examine crestal bone stress and strain.

Conclusions

For this in vitro model system,

1. All abutment types and locations around the implant showed axially loaded generated strains in the peri-implant region that fell within or below the physiologic zone for cancellous bone remodeling, which is 200–2500 με.
2. With the UCLA abutment, the highest strains occurred in the peri-implant region (596 με), while the cemented abutment type showed the lowest strain distribution (386.41 με), and the 2-screw abutment type showed strains between the other abutment types (462.4 με).
3. With axial loading, little difference was observed in the strain distribution in the peri-implant region on the facial, mesial, and distal sides of the implant.

Abbreviations

GLM: general linear model

PMMA: polymethylmethacrylate

References

1. Esposito M, Grusovin MG, Willings M, Coulthard P, Worthington HV. The effectiveness of immediate, early and conventional loading of dental implants: a Cochrane systematic review of RCTs. *Int J Oral Maxillofac Implants*. 2007;22:893–904.

2. Assenza B, Scarano A, Petrone G, Iezzi G, Thams U, San Roman F,

Piattelli A. Crestal bone remodeling in loaded and unloaded implants and the microgap: a histologic study. *Implant Dent*. 2003;12:235–241.

3. Oh TJ, Yoon J, Misch CE, Wang HL. The cause of early implant bone loss: myth or science? *J Periodontol*. 2002;73:322–337.

4. Piao CM, Lee JE, Koak JY, et al. Marginal bone loss around three different implant systems: radiographic evaluation after 1 year. *J Oral Rehabil*. 2009;36:748–754.

5. Hoshaw SJ, Brunski JB, Cochran GVB. Mechanical loading of Branemark implants affects interfacial bone modeling and remodeling. *Int J Oral Maxillofac Implants*. 1994;9:345–360.

6. Hekimoglu C, Anil N, Cehreli MC. Analysis of strain around endosseous dental implants opposing natural teeth or implants. *J Prosthet Dent*. 2004;92:441–446.

7. Bobyn JD. Producing and avoiding stress shielding. *Clin Orthop*. 1990;261:196–211.

8. Ishigaki S, Nakano T, Yamada S, et al. Biomechanical stress in bone surrounding an implant under simulated chewing. *Clin Oral Implants Res*. 2003;14:97–102.

9. Lekholm U, Gunne J, Henry P. Survival of Branemark implants in partially edentulous jaws: a 10-year prospective multicenter study. *Int J Oral Maxillofacial Implants*. 1999;14:639–645.

10. Vaillancourt H, Pilliar RM, McCammond D. Finite element analysis of crestal bone loss around porous coated dental implants. *J Appl Biomaterials, Part B*. 1995;6:267–282.

11. Proff P, Romer P. The molecular mechanism behind bone remodeling: a review. *Clin Oral Investig*. 2009;13:355–362.

12. Martin RB, Burr DB. *Structure, Function and Adaptation of Compact Bone*. New York, NY: Raven Press; 1989.

13. Frost HM. Transient-steady state phenomena in microdamage physiology: a proposed algorithm for lamellar bone. *Calcif Tissue Int*. 1989; 44:367–381.

14. Mori S, Burr DB. Increased intracortical remodeling following fatigue damage. *Bone*. 1993; 14:103–109.

15. Hoshaw SJ, Brunski JP, Cochran GVB. Mechanical loading of Branemark implants affects interfacial bone modeling and remodeling. *Int J Oral Maxillofac Implants*. 1994;9:345–360.

16. Frost HM. Bone histomorphometry: choice of marking agent and labeling schedule. In: Recker RR, ed. *Bone Histomorphometry: Techniques and Interpretation*. Boca Raton, Fla: CRS Press, 1983:37–52.

17. Tabata LF, Rocha EP, Barão VA, Assunção WG. Platform switching: biomechanical evaluation using three-dimensional finite element analysis. *Int J Oral Maxillofac Implants*. 2011;22:482–491.

18. Vaillancourt H, Pillar R, McCammond D. Factors affecting crestal bone loss with dental implants partially covered with a porous coating: a finite element analysis. *Int J Oral Maxillofac Implants*. 1996;11:351–359.

19. Choi K, Kuhn JL, Ciarelli MJ, Goldstein SA. The elastic moduli of human subchondral trabecular and cortical bone tissue and the size-dependency of cortical bone modulus. *J Biomech*. 1990;23:1103–1113.

20. Lotz JC, Gerhart TN, Hayes WC. Mechanical properties of metaphyseal bone in the proximal femur. *J Biomech*. 1989;24:317–329.

21. McElhaney JH, Fogel JI, Melvin JW, Hayne RR, Roberts VL, Alem NM. Mechanical properties of cranial bone. *J Biomech*. 1970;3:495–511.

22. Murry RP, Hayes WC, Edwards WT, Harry JD. Mechanical properties of subchondral plate and the metaphyseal shell. *Trans 30th Orthop Res Soc*. 1984;9:197.

23. Clelland NL, Gilat A. The effect of abutment angulation on stress transfer for an implant. *J Prosthod*. 1992;1:24–28.

24. Jaffin RA, Berman CL. The excessive loss of Branemark fixtures in Type IV bone: a 5-year analysis. *J Periodontol*. 1991;62:2–4.

25. Clelland NL, Papazoglou E, Carr AB, Gilat A. Comparison of strains to a bone simulated among implant overdenture bars with various levels of misfit. *J Prosthodont*. 1995; 4:243–250.

26. Dally JW, Rilley WF. *Experimental Stress Analysis*. 3rd ed. New York, NY: McGraw-Hill; 1991.

27. Muller F, Hemandez M, Grutter L, Aracil-Kessler L, Weingert D, Schimmel M. Masseter muscle thickness, chewing efficiency and bite force in edentulous patients with fixed and removable implant-supported prostheses: a cross-sectional multicenter study. *Clin Oral Implants Res*. 2012;23:144–150.

28. Tukey JW, Mostler F, Hoaglin DC. *Understanding Robust and Exploratory Data Analysis*. New York, NY: Wiley Inc; 1983.

29. Rubin CT, Lanyon LE. Osteoregulatory nature of mechanical stimuli as a determinant for adaptive remodeling in bone. *J Orthop Res*. 1987;5:300–309.

30. Baca E, Yengin E, Gökçen-Röhlig B, Sato S. In vivo evaluation of occlusal contact area and maximum bite force in patients with various types of implant-supported prostheses. *Acta Odontol Scand*. 2013;71:1181–1187.

31. Fu JH, Hsu YT, Wang HL. Identifying occlusal overload and how to deal with it to avoid marginal bone loss around implants. *Eur J Oral Implantol*. 2012;5(suppl):S91–S103.

32. Lindquist LW, Carlsson GE. Long-term effects on chewing with mandibular fixed prostheses on osseointegrated implants. *Acta Odontol Scand*. 1985;43:39–45.

33. Luraschi J, Schimmel M, Bernard JP, Gallucci GO, Belser U, Müller F. Mechanosensation and maximum bite force in edentulous patients rehabilitated with bimaxillary implant-supported fixed dental prostheses. *Clin Oral Implants Res*. 2012;23:577–578.

34. Svensson KG, Trulsson M. Impaired force control during food holding and biting in subjects with tooth- or implant-supported fixed prostheses. *J Clin Periodontol*. 2011;38:1137–1146.

35. Jacques LB, Moura MS, Suedam V, Souza EA, Rubo JH. Effect of cantilever length and framework alloy on the stress distribution of mandibular-cantilevered implant-supported prostheses. *Clin Oral Implants Res*. 2009;20:737–741.

36. Kinni ME, Hokanna SN, Caputo AA. Force transfer by osseointegration implant devices. *Int J Maxillofac Implants*. 1987;2:11–14.

37. Haraldson TA. A photoelastic study of some biomechanical factors affecting the anchorage of osseointegrated implants in the jaw. *Scand J Plast Reconstr Surg*. 1980;14:209–214.

38. Soltesz U, Siegele D, Riedmuller J, Schulz P. Stress concentration and bone resorption in the jaw for dental implants with shoulders. In: Lee AJC, Albrektsson T, Branemark PI, eds. *Clinical Applications of Biomaterials*. New York, NY: Wiley; 1982:115–122.

39. Borchers L, Reichart P. Three-dimensional stress distribution around a dental implant at different stages of interface development. *J Dent Res*. 1983;63:155–159.

40. Cook SD, Klawittter JJ, Weinstein AJ, Lavernia CJ. The design and evaluation of dental implants with finite element analysis. In: Gallagher RA, ed. *Finite Elements in Biomechanics*. Tucson: University of Arizona; 1980:169–178.

41. Misch CE, Ismail YH, Ibiari W. Stress analyses of two blade implants with increased width and length of their neck portions [abstract #67]. *J Dent Res*. 1990;69:117.

42. Misch CE. *Contemporary Implant Dentistry*. St. Louis, Mo: CV Mosby Inc; 1993:19–28.

43. Pillar RM. Radiographic and morphologic studies of load-bearing porous-surfaced structured implants. *Clin Orthop*. 1981:156:249–257.

44. Weinberg LA. The biomechanics of force distribution in implant supported prostheses. *Int J Oral Maxillofac Implants*. 1993;8:19–31.

45. Brennan JG, Jowitt R, Mughsi OA. Some experience with the General Foods Texturometer. *J Texture Stud*. 1970;6:167–189.

46. Wang JS, Stohler CS. Textural properties of food used in studies of mastication. *J Dent Res*. 1990;69:1546–1550.

47. Kaukinen JA, Edge MJ, Lang BR. The influence of occlusal design on simulated masticatory forces transferred to implant-retained prosthesis and supporting bone. *J Prosthet Dent*. 1996;76:50–55.

48. Park JB, Lakes RS. *Biomaterials: An Introduction*. 2nd ed. New York, NY: Plenum Press; 1992.